

FAILURE SIMULATION OF FIBER REINFORCED CONCRETE BEAMS SUBJECTED TO DYNAMIC LOADINGS

KUNHWI KIM* AND YUN MOOK LIM†

*University of California, Davis
One Shields Ave., Davis, CA 95616, USA
e-mail: khtkim@ucdavis.edu

†Yonsei University
50 Yonsei-ro, Seodaemun-gu, Seoul 120-749, Korea
e-mail: yunmook@yonsei.ac.kr

Key words: Fiber Reinforced Cementitious Composites, Dynamic Failure, Irregular Lattice Model, Rate Dependency

Abstract. The dynamic failure behavior of fiber reinforced cementitious composites (FRCC) is simulated using an irregular lattice model. During fracture process, the visco-plastic contributions represent the rate dependency of the matrix phase. Individual fibers are introduced within the lattice framework for the explicit modeling of these heterogenous features of the composites. Three-point bending tests are simulated for a plain mortar beam and FRCC beams with two different fiber volume fractions. Crack patterns and load responses are presented for the evaluation of failure characteristics. The results provide qualitative understandings of the failure features of FRCC structures under dynamic loading conditions.

1 INTRODUCTION

In the design of infrastructure facilities and other critical structures, increasing emphasis is being given to their resistance to extreme dynamic events, such as earthquakes, impacts, and blasts. Fiber reinforced cementitious composites (FRCC) are appropriate for meeting such performance requirements, due to their superior toughness relative to ordinary concrete. Accordingly, much experimental research has been conducted on fracture behavior of FRCC under various dynamic conditions [1–4].

The relevance of modeling becomes even more important when considering structural performance under dynamic loadings, due to the expense and complications of testing at larger scales. Recently, numerical investigations have been conducted on dynamic failure

behavior of fiber reinforced concrete subjected to various loading conditions [5, 6]. These simulations adopted constitutive relations in which the composite material is regarded as a homogeneous continuum.

As apposed to the above numerical schemes, the inclusion of fibers can be modeled within discrete frameworks. Bolander et al. [7, 8] introduced an explicit modeling of fibers within the rigid-body-spring network (RBSN), which effectively represents the pre- and post-cracking contributions of individual fibers to the composite behavior. Cusatis et al. [9, 10] improved the lattice discrete particle model (LDPM) framework for modeling micro-mechanical fiber-matrix interaction including matrix spalling, bending and snubbing of fibers during fiber pull-out.

In this study, dynamic failure behavior of

FRCC is simulated by a lattice model based on the RBSN framework. Simulations of three-point bending tests are conducted for the cases of plain mortar and two different volume fractions of fibers. Failure characteristics of each beam are evaluated through their crack patterns and load responses.

2 MODEL CONSTRUCTION

2.1 Lattice modeling of FRCC

The lattice representing the matrix phase is modeled through the Delaunay-Voronoi tessellations of the material domain. Two neighboring rigid cells i and j interconnect via a spring set, which consists of normal, tangential, and rotational springs in local $n-t$ coordinates with elastic stiffness coefficients k_n , k_t , and k_ϕ , respectively (Fig. 1). The fracture properties are described by degrading the strengths and stiffnesses of springs according to the fracture criteria [11]. During fracture process, rate dependent features are described by a visco-plastic rheological component incorporated in the matrix element. Details of element formulation and calibration of the visco-plastic model can be found in [11].

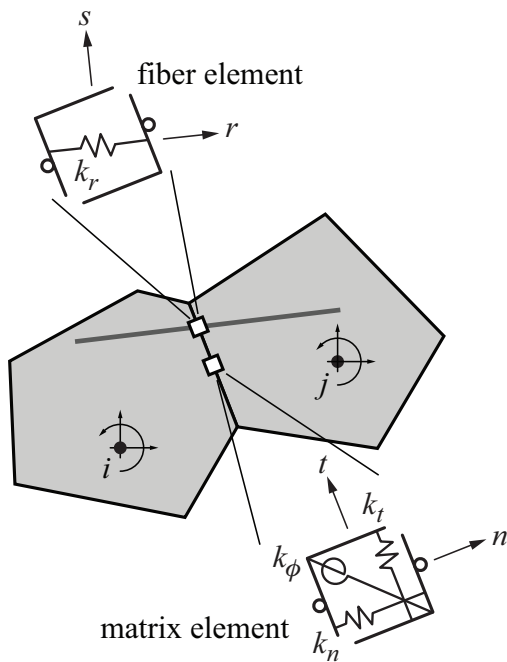


Figure 1: Two-cell assembly of a lattice element with fiber inclusion.

Fibers are explicitly represented as additional spring elements within the lattice model, irrespective of the discretization of the matrix elements. A fiber element is composed of an axial spring along local r -axis (see Fig. 1), and the stiffness coefficient k_r is assigned by assuming perfect bonding between the fiber and matrix before cracking of the matrix element. Stiffness contribution of the fiber element is transferred to the degrees of freedom of nodes i and j . Therefore, the fiber elements do not increase the number of system degrees of freedom, which enables consideration of realistically large numbers of fibers [8].

After cracks initiate within the matrix phase, the spring properties of fiber elements that cross the cracks are modified according to the mechanisms of debonding and frictional pull-out. The pull-out curves are derived from the parameters associated with the bond stress-slip relations and the embedded fiber lengths. As shown in Fig. 2, the pull-out load is simplified as parabolically ascending-linearly descending with increasing slip displacement. The maximum pull-out load P_f at full debonding displacement δ_0 can be derived as $P_f = (\pi d_f l_e) \tau_f$, where d_f is the fiber diameter, l_e is the embedded length, and τ_f is the frictional bond strength of the interface. Tensile rupture of the fiber can be modeled, as it depends on fiber axial stress, but this factor is not considered in this study.

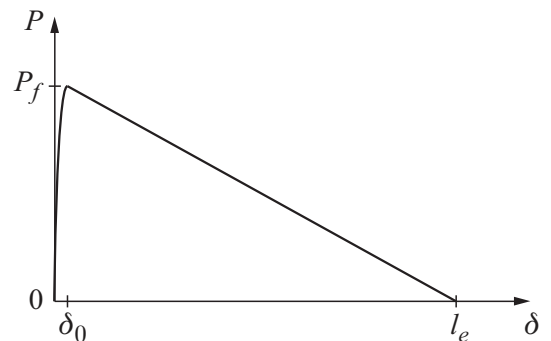


Figure 2: Pull-out load versus slip displacement for a fiber.

2.2 Composition of specimens

The lattice model is applied to simulate the three-point bending test illustrated in Fig. 3.

The beam specimen is 12.5 mm in depth, 300 mm in length, and 75 mm in thickness. For loading conditions, a uniform velocity of 100 mm/s is imposed on the 250 mm span length, which corresponds to the flexural strain rate of 0.12 /s.

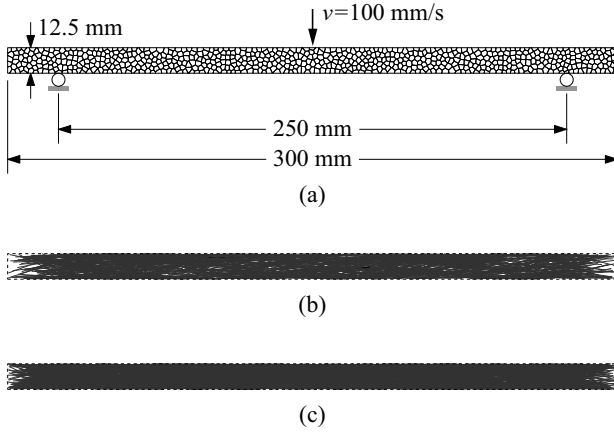


Figure 3: Modeling of beam specimen: (a) Voronoi cell discretization and loading configuration; (b) 1145 fibers for $V_f = 0.5\%$; (c) 2291 fibers for $V_f = 1.0\%$.

Mortar properties are given to characterize the lattice elements for the matrix phase: density $\rho = 2160 \text{ kg/m}^3$; elastic modulus $E = 34.8 \text{ GPa}$; tensile strength $f_t = 6.7 \text{ MPa}$; and fracture energy $G_F = 80 \text{ N/m}$. The visco-plastic parameters are calibrated to represent the appropriate increase of dynamic strength from rate effects, using a procedure outlined in [11].

Steel fibers are uniformly distributed with randomly generated positions and orientations in the specimen domain (Fig. 3b and c). The dimensions of an individual fiber are: diameter $d_f = 0.25 \text{ mm}$; and length $l_f = 25.0 \text{ mm}$. The number N_f of fibers introduced in the model can be determined as $N_f = \text{INT}[4V_fV/(\pi d_f^2 l_f)]$, where V is the volume of specimen domain and V_f is a fiber volume fraction. In this study, FRCC beams with $V_f = 0.5\%$ and 1.0% are tested as well as a plain mortar beam ($V_f = 0\%$). The fiber elements have elastic modulus $E_f = 200 \text{ GPa}$; and tensile rupture strength $f_r = 620.5 \text{ MPa}$, adopted from [1]. The bond strength τ_f is assumed to be the same as the tensile strength f_t of the matrix.

3 RESULTS AND DISCUSSION

The resulting data are obtained from the simulations up to a midspan deflection of 3.5 mm, which is assumed to represent failure. To evaluate the fiber reinforcing effects on the composite failure behavior, crack patterns and load-deflection responses are presented for the considered fiber volume fractions $V_f = 0.5\%$ and 1.0% including plain mortar.

3.1 Crack patterns

Fig. 4 shows crack patterns of the deformed specimens at the assumed failure stage. For improved visibility of crack formations, the displacements are magnified and cracked facets are traced by bold lines. A single crack initiates and develops near midspan of the plain mortar beam (Fig. 4a), whereas multiple cracks are distributed along the FRCC beams (Fig. 4b and c). The higher fiber volume fraction extends the multi-cracked region with smaller crack openings, which indicates a more ductile failure behavior.

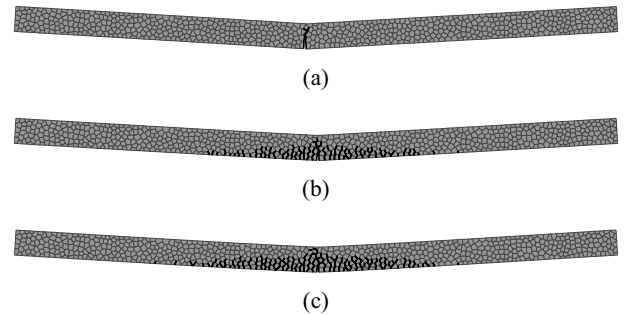


Figure 4: Crack patterns for (a) plain mortar, (b) $V_f = 0.5\%$, and (c) $V_f = 1.0\%$.

3.2 Load-deflection responses

Load responses versus the midspan deflections are presented in Fig. 5. The support reactions are acquired at every loading step and added up as the load resistance. The simulated responses from original data exhibit much fluctuation due to the wave propagation within the specimen; the curves are plotted after filtering and smoothing processes to reduce the noises.

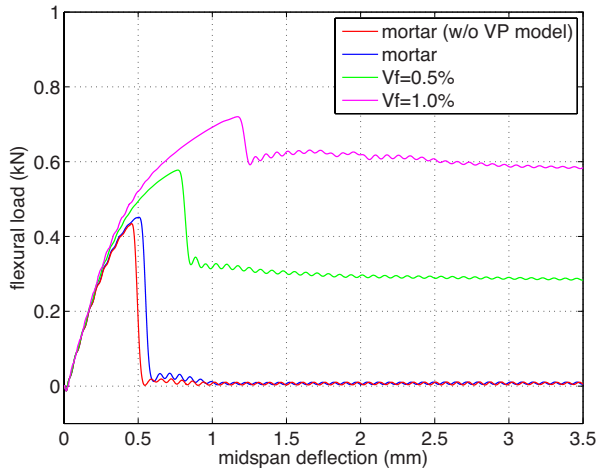


Figure 5: Load-deflection curves for beam specimens.

The plain mortar beam shows a rapid dissipation of the load resistance after the crack occurs. In contrast, the FRCC beams exhibit hardening in the load response with higher load-carrying capacity during multi-cracking of the matrix elements. The load response is decreased after fracture is localized, but the fiber pulling-out provides ductility in the composite softening behavior. The greater volume fraction of fibers involves fracture localization at the larger deflection and the higher load retained in the softening behavior.

An additional simulation without the visco-plastic model is conducted for the plain mortar beam, and the resulting load response is also plotted Fig. 5. Compared to the load response simulated with the visco-plastic model, it shows a lower load-carrying capacity and load reduction at less deflection. The difference in the response curves is not large due to the relatively low loading rate considered. This comparison of the results indicates that the enhancement of properties due to the material rate dependency is implemented by the visco-plastic model.

Note that rate dependency of fiber-matrix interfacial behavior is not considered within the current model, but it should be addressed in further studies. In reality, the pull-out behavior of fibers is quite dependent on the strain (loading) rates, but the extent of rate sensitivity is differentiated by the material and the shape

of fibers [12, 13]. Parametric studies will be needed to represent the rate dependent interfacial properties for various fiber types.

4 CONCLUSIONS

An irregular lattice model framework is used to study the dynamic failure behavior of FRCC structures. The elastic and fracture properties of the matrix phase are represented by the RBSN model, and the rate effects during fracture process can be described by the visco-plastic elements incorporated in the lattice springs. The explicit modeling of fiber inclusion enables a realistic representation of FRCC based on physical mechanisms of fiber-matrix interactions.

Three-point bending tests are simulated for the plain mortar and FRCC beams. In the simulation results, ductile failure features, such as the formation of multiple cracks and the enhanced load resistance, are observed and qualitatively compared for different fiber volume fractions. Also, the rate dependency of the matrix fracture is verified in terms of the flexural strength.

Although the current fiber model does not account for the rate dependency of interfacial properties, preliminary results show the capability to simulate the dynamic fracture of FRCC. With improvements in the constitutive model, this modeling approach can be used to analyze the rate dependent failure of FRCC.

REFERENCES

- [1] Naaman, A.E. and Gopalaratnam, V.S., 1983. Impact properties of steel fibre reinforced concrete in bending. *Int. J. Cem. Compos. Lightweight Concrete* **5**(4):225–233.
- [2] Banthia, N., Chokri, K., Ohama, Y. and Mindess, S., 1994. Fiber-reinforced cement based composites under tensile impact. *Adv. Cem. Based Mater.* **1**:131–141.
- [3] Lok, T.S. and Zhao, P.J., 2004. Impact response of steel fiber-reinforced concrete using a split Hopkinson pressure bar. *J. Mater. Civ. Eng.* **16**(1):54–59.

- [4] Mechtcherine, V., Millon, O., Butler, M. and Thoma, K., 2011. Mechanical behaviour of strain hardening cement-based composites under impact loading. *Cem. Conc. Compos.* **33**(1):1–11.
- [5] Teng, T.L., Chu, Y.A., Chang, F.A., Shen, B.C. and Cheng, D.S., 2008. Development and validation of numerical model of steel fiber reinforced concrete for high-velocity impact. *Comp. Mater. Sci.* **42**:90–99.
- [6] Wang, Z.L., Wu, L.P. and Wang, J.G., 2010. A study of constitutive relation and dynamic failure for SFRC in compression. *Constr. Build. Mater.* **24**:1358–1363.
- [7] Bolander, J.E. and Sukumar, N., 2005. Irregular lattice model for quasistatic crack propagation. *Phys. Rev. B* **71**, 094106.
- [8] Bolander J.E., Choi, S. and Duddukuri, S.R., 2008. Fracture of fiber-reinforced cement composites: effects of fiber dispersion. *Int. J. Fract.* **154**(12):73–86.
- [9] Cusatis, G., Schaufert, E.A., Pelessone, D., O’Daniel, J.L., Marangi, P., Stacchini, M. and Savoia, M., 2010. Lattice discrete particle model for fiber reinforced concrete (LDPM-F) with application to the numerical simulation of armor-ing systems. In Bićanić et al. (eds), *Proc. of Computational Modelling of Concrete Structures (EURO-C 2010)*, March 15-18, 2010, Rohrmoos/Schladming, Austria; pp. 291-300.
- [10] Schaufert, E.A. and Cusatis, G., 2012. Lattice discrete particle model for fiber-reinforced concrete. I: Theory. *J. Eng. Mech.* **138**(7):826–833.
- [11] Kim, K. and Lim, Y.M., 2011. Simulation of rate dependent fracture in concrete using an irregular lattice model. *Cem. Conc. Compos.* **33**(9):949–955.
- [12] Gokoz, U.N. and Naaman, A.E., 1981. Effect of strain-rate on the pull-out behaviour of fibres in mortar. *Int. J. Cem. Compos.* **3**(3):187–202.
- [13] Kim, D.J., El-Tawil, S. and Naaman, A.E., 2008. Loading rate effect on pullout behavior of deformed steel fibers. *ACI Mater. J.* **105**(6):576–584.